

DIGITAL APPROACH TO THERMIONIC EMISSION CURRENT TO VOLTAGE CONVERSION FOR HIGH-VOLTAGE SOURCES OF ELECTRONS

Bartosz Kania

Lublin University of Technology, Department of Automatics and Metrology, Lublin, Poland

Abstract. The thermionic emission current is used in many vacuum devices such as evaporators, rare gas excimers, or electron beam objects for high-energy physics. The stability of the thermionic emission current is a very important requirement for the accuracy of those devices. Hence, there is a number of control systems that use a feedback signal directly proportional to the emission current in order to stabilize the thermionic emission current. Most of them use feedback from a high-voltage anode circuit to a low-voltage cathode circuit. However, there is a novel solution that uses linear cathode current distribution and processing of two cathode circuit voltage signals for converting the emission current to voltage. However, it is based on old-fashioned analog technology. This paper shows the thermionic emission current to voltage conversion method with the use of a digital control system. A digital realization of a multiplicative-additive algorithm is presented and proper work in closed-loop mode is confirmed.

Keywords: electron emission, electron sources, control system synthesis, digital control

CYFROWE PODEJŚCIE DO METODY KONWERSJI NATEŻENIA PRĄDU TERMOEMISJI ELEKTRONOWEJ NA NAPIĘCIE DLA WYSOKONAPIĘCIOWYCH ŹRÓDEŁ ELEKTRONÓW

Streszczenie. Prąd termoemisji elektronowej jest wykorzystywany w wielu przyrządach próżniowych takich jak ewaporatory, ekscymery gazów rzadkich czy w fizyce wysokich energii. Stabilność natężenia prądu termoemisji elektronowej jest ważnym wymaganiem w kontekście dokładności tych przyrządów. Istnieje wiele układów regulacji natężenia prądu termoemisji elektronowej, które używają sygnału sprzężenia zwrotnego wprost proporcjonalnego do natężenia prądu termoemisji elektronowej w celu jego stabilizacji. Większość z nich wykorzystuje sprzężenie od wysokonapięciowego obwodu anody do niskonapięciowego obwodu katody. Istnieje nowe rozwiązanie, które wykorzystuje liniowy rozkład prądu katody oraz przetwarzanie dwóch sygnałów z obwodu katody w celu konwersji natężenia prądu termoemisji na napięcie. Niestety metoda ta bazuje na przestarzałej technologii analogowej. W niniejszej pracy pokazana została konwersja natężenia prądu termoemisji elektronowej na napięcie z użyciem cyfrowego układu automatycznej regulacji. Cyfrowa realizacja algorytmu multiplikatywno-addytywnego została zaprezentowana, a poprawna praca w zamkniętej pętli sprzężenia zwrotnego potwierdzona.

Słowa kluczowe: emisja elektronów, źródła elektronów, synteza systemu sterowania, sterowanie cyfrowe

Introduction

There are many vacuum devices that use thermionic electron sources operating under temperature or space charge limited mode, such as electron beam objects for high energy physics [17], water radiolysis [21], [23] integrated circuit manufacturing process monitors [16], X-ray photoelectron spectrometers [22], devices producing rare gas excimers [3] or evaporators [15]. The stability of the electron emission current is one of the most important requirements for electron sources. Most thermionic emission current stabilizers use negative feedback loop control systems where thermionic emission current is measured in a high-voltage anode supply circuit [1, 4–10, 12, 14, 15, 18, 19] and transferred to a low-voltage cathode supply circuit. For relatively low values of electron accelerating voltage both, the cathode and the anode circuits, can be at a common electric potential. However, for higher values of electron accelerating voltage, some modifications are needed due to the limited breakdown voltage of semiconductor components, such as optical isolation [15], [8], in order to safe signal transfer between the anode and the cathode circuit.

An impediment to transferring feedback signal in high-voltage electron sources was a ground for a novel solution using cathode circuit currents measurements to convert emission current into voltage [13]. This solution offers relatively high conversion accuracy for low values of the electron work function of the cathode material. However, it bases on old-fashioned analog technology. This paper shows the thermionic emission current to voltage conversion method with the use of a digital control system. An implementation of a digital algorithm is presented, and proper work in closed-loop mode is confirmed.

1. Hardware design

A block diagram of control system hardware is presented in Fig. 1. The control system hardware consists of several main hardware components:

- a PC with the Windows operating system and LabVIEW scientific and engineering software from National Instruments,

- NI USB-6251 data acquisition card from National Instruments,
- the main electronic system processing measurement and control signals,
- controlled system – a hot cathode electron source.

A PC is a platform for control algorithms implemented in the LabVIEW environment. The algorithm's more detailed description is in the next section below. The data acquisition card [24] offers 8 differential inputs or 16 inputs operating in the common potential mode with a resolution of 16 bits. The maximum sampling rate is 1.25 MS/s for single-channel operation or 1 MS/s for multi-channel operation. In addition, the card offers 2 analog outputs with a resolution of 16 bits and a sampling frequency of 2.86 MS/s for single-channel operation and 2 MS/s for two-channel operation. The analog inputs of measuring amplifiers of the data acquisition card were used in the differential configuration ensuring the reduction of the common signal at the outputs.

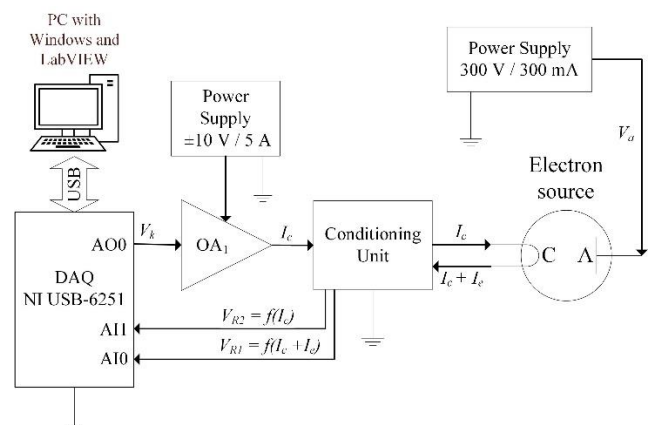


Fig. 1. A block diagram of control system hardware. OA_1 is the high-current operational amplifier OPA 549, V_a is the anode supply voltage, V_k is the cathode circuit supply voltage, V_{R1} and V_{R2} are voltage drops across sensing resistors R_1 and R_2 in the cathode circuit, I_e is a process value of the electron emission current, I_c is the cathode heating current, C means the cathode, A means the anode

The center of the test stand is an electronic system designed to process measurement and control signals. There are 2 circuits: cathodes one and anodes one.

Fig. 2 shows a schematic diagram of the electronic system. The cathode power supply voltage V_k is fed to the cathode through the operational power amplifier OA_1 (OPA549, Texas Instruments) with a voltage gain of 1.2 V/V. The current in the cathode circuit also flows through the sensing resistors R_1 and R_2 . The signal V_a fed from power supply unit constitutes the control voltage of the anode. The emission current flows through the anode, the cathode, and the resistor R_1 to the ground of the system.

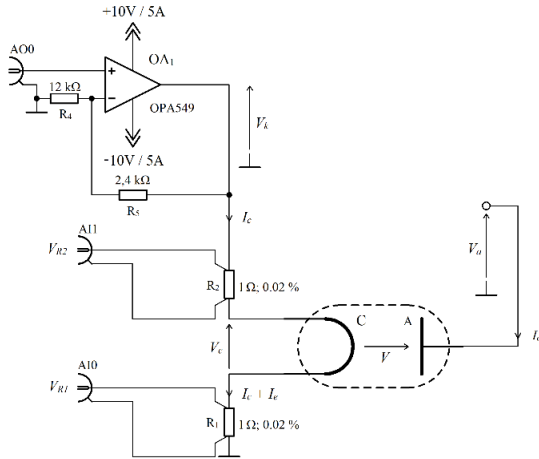


Fig. 2. Detailed control system hardware diagram. Controlling signals: V_k is the cathode power supply voltage, V_c is the cathode voltage, V_a is the anode supply voltage; V_{R1} and V_{R2} are voltage drops across sensing resistors R_1 and R_2 , respectively; A10 and A11 are analog inputs of the data acquisition card, A00 is analog output of the data acquisition card

The system uses two sensing resistors VPR221 (Vishay Foil Resistors) [25] with a resistance of 1 Ω , tolerance $\pm 0.02\%$, maximum temperature coefficient of ± 5 ppm/ $^{\circ}\text{C}$, and power of 8 W each. They are connected in series in the cathode circuit: the resistor R_2 between the control voltage source V_k and the cathode terminal; the resistor R_1 between the other cathode terminal and the common reference potential – the ground of the system. According to the analysis presented in [13], the potential drop across the resistor R_2 is directly proportional to the cathode heating current I_c

$$V_{R2} = R_2 I_c \quad (1)$$

while the potential drop across the resistor R_1 is directly proportional to the sum of the currents flowing through the resistor.

$$V_{R1} = R_1 (I_c + I_e) \quad (2)$$

Voltage signals from the terminals of the resistors are fed to the inputs of the data acquisition card, where they are subjected to analog-to-digital conversion. A high-voltage power supply in the anode circuit supplies energy to the anode.

2. Algorithm

Data acquisition, analysis, and control algorithm are implemented with the use of a PC with Windows operating system and LabVIEW (National Instruments) environment. The algorithm is presented in Fig. 3.

The algorithm begins with the initialization of the data acquisition card. Moreover, the following properties are configured: the source of the clock signal (internal clock signal), the type of measurement (differential), the range of input values (0 – 2 V or 0 – 10 V), and the sampling frequency (250 kSPS). The next part of the process is reading the input signals. The collected measurement data contains a noise signal. Therefore, as part of digital processing, the data is averaged over the iteration period of the algorithm, and then transformed according to assumption $R = R_1 = R_2$ and formula (3).

$$I_e = \frac{V_{R1} - V_{R2}}{R} \quad (3)$$

The iteration period of the algorithm was determined as – Fig. 3.

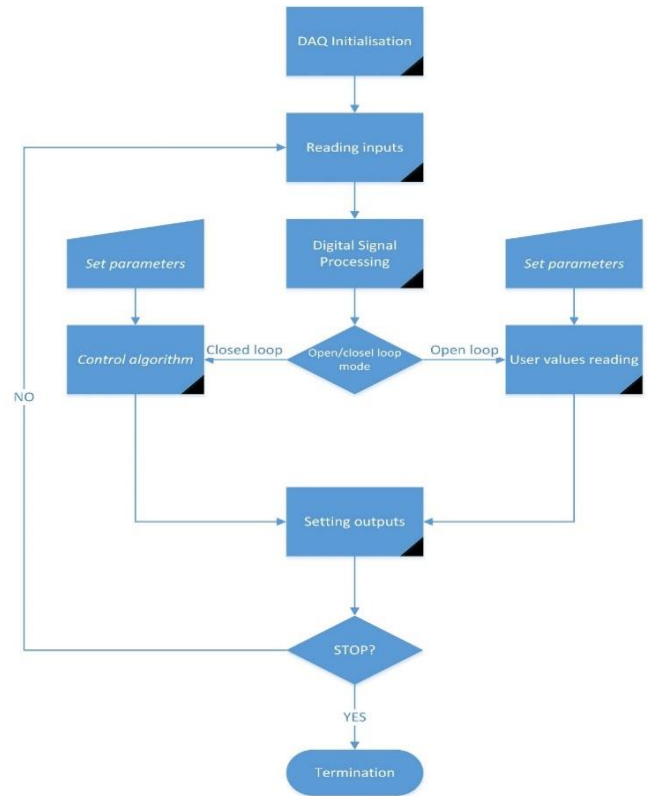


Fig. 3. The algorithm diagram

$$T_s \cong \frac{1}{12} T_{95} \cong 100 \text{ ms} \quad (4)$$

where T_s is the iteration period of the control algorithm, and T_{95} is the settling time (until the step response reaches 95% of the set value). Then, depending on the active mode, the value of the control signal is calculated with the use of given parameters (closed feedback loop) or the data, such as the cathode circuit supply voltage V_k' , is taken from an user (open feedback loop). In the case of the closed-loop operation, the user has to determine the reference value of the electron emission current I_{eref} . Next, the output signals of the data acquisition card are updated. At this point, the control process can be completed, or the cycle starts again, i.e. reading the input signals.

A block diagram of the developed of the electron emission current control system is presented in Fig. 4.

As one can see, the controlled system covers two input signals and three output signals. The thermionic electron source has a higher-order inertia nature [20], [11]. Taking into account small signal transconductance $G(s)$ [13]

$$G(s) = \frac{G_0}{T_c s + 1} e^{-sT_0} \quad (5)$$

where G_0 is the DC transconductance, T_c is the time constant, T_0 is the delay time, s is the Laplace operator, and the equation derived in [13], which describes electron accelerating voltage V

$$V = V_a - \frac{1}{3} R_c I_e - \frac{1}{2} R_c I_c \quad (6)$$

where R_c is the resistance of the cathode; the controlled system transfer function $\mathbf{H}(s)$ (see Figure 4) can be described as a series of two transfer functions, $\mathbf{H}_1(s)$ and \mathbf{H}_2 :

$$\mathbf{H}_1(s) \begin{bmatrix} I_e \\ I_c \end{bmatrix} = \begin{bmatrix} \frac{G_0}{T_c s + 1} e^{-sT_0} \\ \frac{1}{R_2 + R_c + R_1} \end{bmatrix} [V_k] \quad (7)$$

$$[V] = \begin{bmatrix} 1 & -\frac{1}{3} R_c + R_1 & -\frac{1}{2} R_c + R_2 \end{bmatrix} \begin{bmatrix} V_a \\ I_e \\ I_c \end{bmatrix} \quad (8)$$

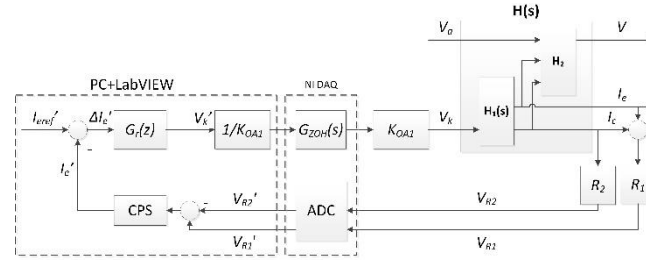


Fig. 4. A block diagram of the electron emission current control system; I_{eref}' is the digital set value of the electron emission current, I_e' is the process value of the electron emission current, I_e' is a digital value of the electron emission current, $\Delta I_e'$ is a digital value of an electron emission current error, V_a is the anode supply voltage, V is the accelerating voltage, V_k' is the digital value of the cathode circuit supply voltage, V_k is the cathode circuit supply voltage, I_c is the cathode heating current, $G_c(z)$, $H(s)$ and $G_{ZOH}(s)$ are transfer functions of the controller, the electron source, and digital to analog converters respectively. K_{OA1} is gain of the operational amplifiers OA1. V_{R1} and V_{R2} are the voltage drops across the measurement resistors R_1 and R_2 in the cathode circuit, respectively. V_{R1}' and V_{R2}' are digital values of the voltage drops V_{R1} and V_{R2} , block ADC is an analog to digital converter, block DSP is digital signal processing

3. Results

The controlled system is a hot cathode electron source. A vacuum diode, 1B3-GT type [2], was used for the tests due to the favorable ratio of the thermionic emission current to the heating current. The rated value of the cathode current is 200 mA, at which the value of the thermal emission current is equal to 3.9 mA (the electron accelerating voltage is equal to 60 V). The cathode has the form of a filament and has a length of 6 mm and a diameter of 0.482 mm. The measurements of the emission current and the cathode voltage were made using HP 34461A multimeters. Type B relative standard uncertainty values of voltage V_c and current I_e are less than 0.0028% and 0.03%, respectively. Fig. 5a shows the static characteristic of the investigated electron source, that is thermionic emission current I_e as a function of the cathode voltage V_c for different values of the anode supply voltage V_a and Figure 5b presents the thermionic emission current I_e vs. the anode supply voltage V_a for different values of the cathode current I_c .

The measurements were performed at open-loop control mode, for heating current I_c up to 200 mA, the anode supply voltage V_a up to 65 V, measurements resistors R_1 and R_2 were shortened ($R_1 = R_2 = 0 \Omega$). As one can see in Fig. 5a and Fig. 5b the thermionic emission current is dependent on the cathode voltage V_c and the anode supply voltage V_a . However, for relatively low values of the anode supply voltage ($V_a < 10$ V) and the cathode voltage more than 0.85 V, the electron source operates in the space charge range. Then the thermionic emission current remains approximately constant with the increase of the cathode voltage V_c . For higher values of the anode voltage, the space charge range is more exiguous, and the emission current saturation range is wider.

Fig. 6 presents the difference of voltage drops V_{R1} and V_{R2} across measurement resistors R_1 and R_2 measured by data acquisition card as a function of thermionic emission current I_e and also linear fitting. The linear function can be expressed by the equation

$$V_{R1} - V_{R2} = 0.9993 \cdot I_e - 0.0035 \quad (9)$$

and a correlation coefficient is 0.99998. Relative nonlinearity for emission current higher than 1 mA is lower than 0,01 %.

Fig. 7 shows the 20-minutes relative standard deviation of the thermionic emission current for the closed-loop mode operation of the thermionic emission current control system. The anode voltage is set to 60 V to ensure that the electron source operates outside the space charge area. The average value of all relative standard deviation points is 0.18 % which confirms the satisfactory stabilization of the thermionic emission current and proper work of the control system using I_e - V conversion method in the cathode supply circuit.

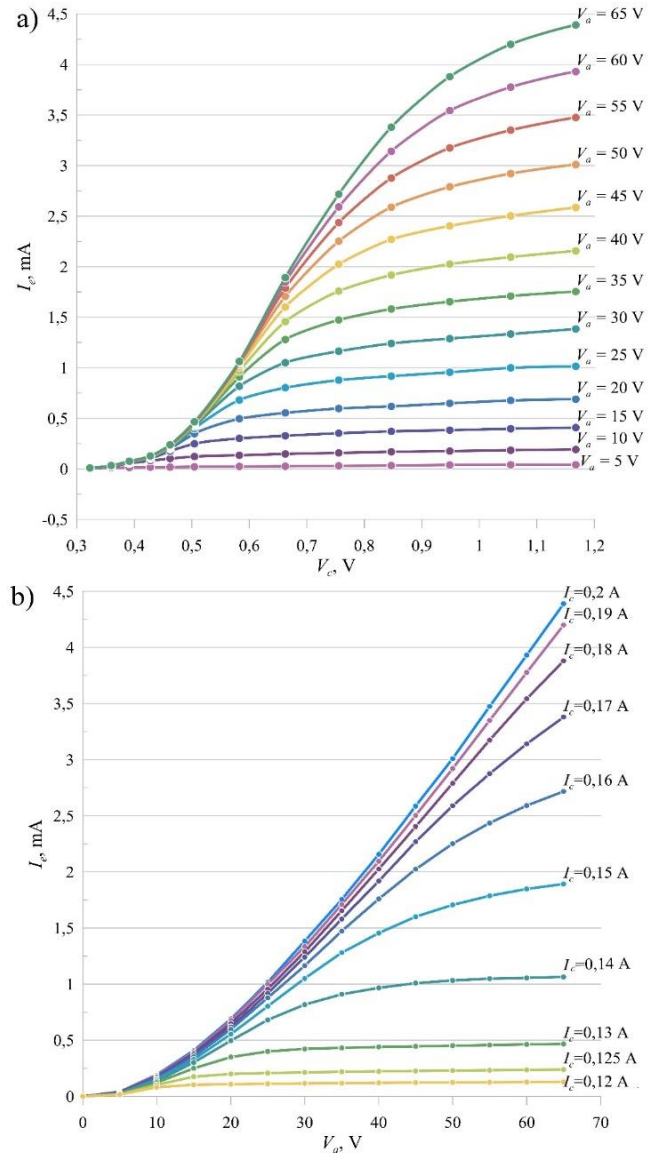


Fig. 5. a) The thermionic emission current I_e vs. the cathode voltage V_c for different values of the anode supply voltage V_a . b) the thermionic emission current I_e vs. the anode supply voltage V_a for different values of the cathode current I_c .

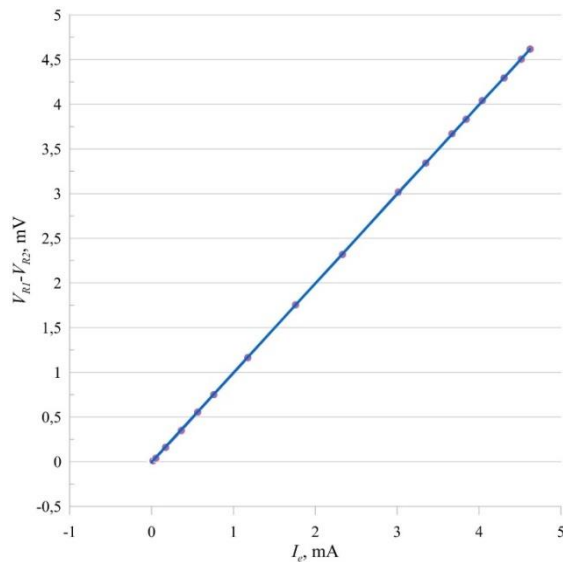


Fig. 6. Difference of voltage drops V_{R1} and V_{R2} across measurement resistors R_1 and R_2 measured by data acquisition card vs. thermionic emission current I_e (dots) and linear fitting (line)

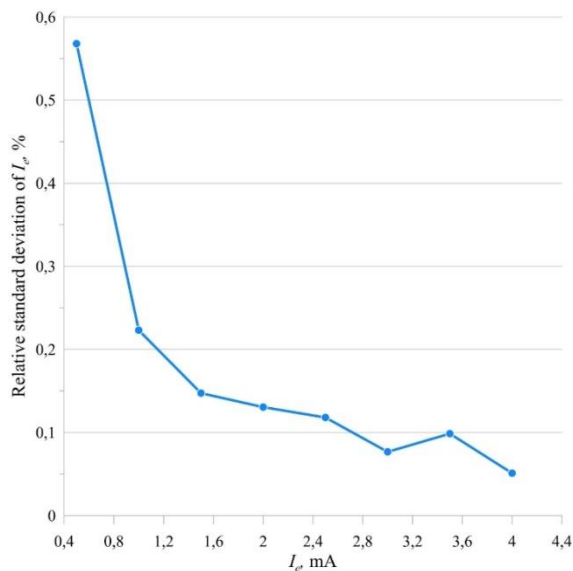


Fig. 7. The 20-minute relative standard deviation of the thermionic emission current I_e for the closed-loop mode operation. The average value of the relative standard deviation is 0.18 %. The anode voltage is 60 V

4. Conclusions

The implementation of the electron emission current to the voltage conversion method in the digital control system was presented. Moreover, the conversion of the emission current to voltage with the use of vacuum diode and sensing resistors in the cathode power supply circuit was successfully tested. The results of experiments with the use of the data acquisition card and digital signal processing of measurement signals confirm high linearity of conversion for more than 1 mA of the thermionic emission current. A relatively high value of the thermionic emission current to the cathode heating current ratio contributes to satisfactory stabilization of the thermionic emission current control system. Moreover, the digital controller is easily tuneable and offers system management or monitoring.

Funding: This research was funded by Lublin University of Technology, Lublin, Science Fund No. FD-20/EE-2/101.

Acknowledgments: The author is thankful to Professor Jarosław Sikora for lots of helpful advices.

References

- [1] Ahn J. et al.: Microprocessor-controlled Electron Impact Ion Source Operated at Constant Discharge Current and Voltage. *Review of Scientific Instruments* 57(3), 1986, 325–328 [http://doi.org/10.1063/1.1138939].
- [2] Angiolillo P.: On Thermionic Emission and the Use of Vacuum Tubes in the Advanced Physics Laboratory. *American Journal of Physics - Amer J Phys* 77, 2009, 1102–1106 [http://doi.org/10.1119/1.3212463].
- [3] Barcellan L. et al.: A Battery-Operated, Stabilized, High-Energy Pulsed Electron Gun for the Production of Rare Gas Excimers. *Review of Scientific Instruments* 82(8), 2011, 095103 [http://doi.org/10.1063/1.3636078].
- [4] Chapman R.: Versatile Wide Range Electron Current Regulator. *Review of Scientific Instruments* 43(10), 1972, 1536–1538 [http://doi.org/10.1063/1.1685484].
- [5] Close K. J., Yarwood J.: A Precision Electron Emission Regulator. *Vacuum* 22(2), 1972, 45–46 [http://doi.org/10.1016/0042-207X(72)90001-2].
- [6] DAQ M Series Manual. National Instruments, 2016.
- [7] Donkov N., Knapp W.: Control of Hot-Filament Ionization Gauge Emission Current: Mathematical Model and Model-Based Controller. *Measurement Science and Technology* 8(7), 1997, 798–803 [http://doi.org/10.1088/0957-0233/8/7/016].
- [8] Durakiewicz T.: Electron Emission Controller with Pulsed Heating of Filament. *International Journal of Mass Spectrometry and Ion Processes* 156(1), 1996, 31–40 [http://doi.org/10.1016/S0168-1176(96)04417-5].
- [9] Flaxer E.: Programmable Smart Electron Emission Controller for Hot Filament. *Review of Scientific Instruments* 82(2), 2011, 025111 [http://doi.org/10.1063/1.3555340].
- [10] Foil Resistors VPR220 & VPR221. Vishay Precision Group, 2014, http://www.vishaypg.com/foil-resistors/list/product-63012/
- [11] Halas S., Sikora J.: Electron Emission Stabiliser with Double Negative Feedback Loop. *Measurement Science and Technology* 1(9), 1990, 980–982 [http://doi.org/10.1088/0957-0233/1/9/023].
- [12] Herbert B. K.: A Circuit for Stabilizing the Electron Current to the Anode of a Hot-Filament Device. *Vacuum* 26(9), 1976, 363–369 [http://doi.org/10.1016/S0042-207X(76)80225-4].
- [13] Kania B., Sikora J.: System Identification of a Hot Cathode Electron Source: Time Domain Approach. *AIP Advances* 8(10), 2018, 105107 [http://doi.org/10.1063/1.5044258].
- [14] Kania B., Sikora J.: Thermionic emission controller with PID algorithm. 23rd International Conference “Mixed Design of Integrated Circuits and Systems” MIXDES 2016, 480–483 [http://doi.org/10.1109/MIXDES.2016.7529790].
- [15] Kuś D. et al.: Conversion Method of Thermionic Emission Current to Voltage for High-Voltage Sources of Electrons. *Electronics* 10(22), 2021, 2844 [http://doi.org/10.3390/electronics10222844].
- [16] Lin X. W. et al.: A Miniature Electron-beam Evaporator for an Ultrahigh-vacuum Atom-probe Field-ion Microscope. *Review of Scientific Instruments* 61(12), 1990, 3745–3749 [http://doi.org/10.1063/1.1141547].
- [17] Meyer zu Heringdorf F. J., Belton A.C.: Flexible Microprocessor-Based Evaporation Controller. *Review of Scientific Instruments* 75(12), 2004, 5288–5292 [http://doi.org/10.1063/1.1818911].
- [18] Oberai A., Jiann-Shiun Y.: Smart E-Beam for Defect Identification & Analysis in the Nanoscale Technology Nodes: Technical Perspectives. *Electronics* 6(4), 2017, 87 [http://doi.org/10.3390/electronics6040087].
- [19] Pepitone K. et al.: Operation of a High-Current Drive Beam Electron Gun Prototype for the Compact Linear Collider. *Review of Scientific Instruments* 91(9), 2020, 093302 [http://doi.org/10.1063/5.0013144].
- [20] Shaw S. Y., Juh T. L.: An Integrated Circuit Based Vacuum Ionisation Gauge Meter. *Journal of Physics E: Scientific Instruments* 13(11), 1980, 1150–1153 [http://doi.org/10.1088/0022-3735/13/11/003].
- [21] Sikora J.: Dual Application of a Biasing System to an Electron Source with a Hot Cathode. *Measurement Science and Technology* 15(1), 2003, N10–14 [http://doi.org/10.1088/0957-0233/15/1/N03].
- [22] Sikora J. et al.: Thermionic Electron Beam Current and Accelerating Voltage Controller for Gas Ion Sources. *Sensors* 21(8), 2021, 2878 [http://doi.org/10.3390/s21082878].
- [23] Siwek M., Edgecock T.: Application of Electron Beam Water Radiolysis for Sewage Sludge Treatment, a Review. *Env. Science and Pollution Research* 27(34), 2020, 42424–42448 [http://doi.org/10.1007/s11356-020-10643-0].
- [24] Stevie F. A., Carrie L. D.: Introduction to X-Ray Photoelectron Spectroscopy. *Journal of Vacuum Science & Technology A* 38(6), 2020, 063204 [http://doi.org/10.1116/6.0000412].
- [25] Zimek Z.: Wytyczne do budowy radiacyjnej instalacji obróbki wód balastowych przy użyciu wiązki elektronów. *Raporty ICHTJ. Seria B nr 2/2020*.

M.Sc. Eng Bartosz Kania
e-mail: b.kania@pollub.pl

He is a graduate of the Faculty of Electrical Engineering and Computer Science of the Lublin University of Technology. In 2013, he began doctoral studies at the Faculty of Electrical Engineering and Computer Science of the Lublin University of Technology in the discipline of Electrical Engineering. He is also a research and lecturer at the Department of Automatics and Metrology of the Lublin University of Technology. Scientific work focuses on the implementation of control algorithms and processing of digital measurement signals.

http://orcid.org/0000-0001-8429-6360

